Developmental Biology xxx (2018) xxx-xxx

Contents lists available at ScienceDirect

Developmental Biology

journal homepage: www.elsevier.com

Developmental atlas of appendicularian *Oikopleura dioica* actins provides new insights into the evolution of the notochord and the cardio-paraxial muscle in chordates

Alba Almazán[1], Alfonso Ferrández-Roldán, Ricard Albalat*, Cristian Cañestro*

Departament de Genètica, Microbiologia i Estadística and Institut de Recerca de la Biodiversitat (IRBio), Facultat de Biologia, Universitat de Barcelona, Av. Diagonal 643, 08028 Barcelona, Catalonia, Spain

ARTICLE INFO

Keywords:
Muscular and cytoplasmic actins
Appendicularian and ascidian urochordates
Chordate evolution
Notochord, heart and paraxial muscle evolution

ABSTRACT

Locomotion by tail beating powered by a system of bilateral paraxial muscle and notochord is likely one of the key evolutionary innovations that facilitated the origin and radiation of chordates. The innovation of paraxial muscle was accompanied by gene duplications in stem chordates that gave rise to muscular actins from cytoplasmic ancestral forms, which acquired contractile capability thanks to the recruitment of the myosin motor-machinery. To better understand the role of actin diversification during the evolution of chordates, in this work we have characterized the complete actin catalogue of the appendicularian *Oikopleura dioica*, an urochordate that maintains a chordate body plan throughout its life, including the notochord in a muscled tail that confers an active free-living pelagic style. Our genomic survey, phylogenetic analyses and Diagnostic-Actin-Values (DAVs) reveal that *O. dioica* has four muscular actins (*ActnM1–4*) and three cytoplasmic actins (*ActnC1–3*), most of which originated by independent gene duplications during the evolution of the appendicularian lineage. Detailed developmental expression atlas of the complete actin catalogue of *O. dioica* reveals differences in the temporal-regulation and tissue-specificity of different actin paralogs, suggesting complex processes of subfunctionalization during the evolution of urochordates. Our results suggest the presence of a "cardio-paraxial" muscular actin at least in the last common ancestor of Olfactores (i.e. vertebrates + urochordates). Our results reveal highly dynamic tissue-specific expression patterns for some cytoplasmic actins, including the notochord, ciliated cells and neurons with axonal projections, which challenge the classic housekeeping notion ascribed to these genes. Considering that previous work had demonstrated the existence of notochord-specific actins in cephalochordates, the tissue-specific expression of two cytoplasmic actins in the notochord of *O. dioica* suggests that this pattern plausibly reflects the ancestral condition of chordates, and provides new insights to better understand the evolutionary origin of the notochord.

1. Introduction

Actins are highly conserved globular proteins, and many of their biological functions derive from their ability to form filaments by linear polymerization (reviewed in Dominguez and Holmes, 2011). Actin microfilaments are one of the major components of the cytoskeleton, being involved in providing structural strength to cellular architecture, ordering and shaping intracellular compartments and organelles, as well as contributing to physically distribute molecules within the cell (Blanchoin et al., 2014; Gunning et al., 2015). Thus, actins have been described to play important roles in cell-cycle control (Heng and Koh, 2010; Tripathi, 1989), chromosome segregation (Ramkumar and Baum, 2016), cell membrane dynamic modulation (Bezanilla et al., 2015; Chang et al., 2017; Fritzsche et al., 2016), regulation of mRNA transport and translation (Besse and Ephrussi, 2008; Vidaki et al., 2017; Zarnack and Feldbrugge, 2010), protein transport and activity modulation (Farwell et al., 1990; Kondrikov et al., 2010; Silva et al., 2016) and regulation of steady-state length of cilia (Avasthi et al., 2014). In addition, the nuclear fraction of actins has been involved in the maintenance of the architecture of the nucleus (Hofmann, 2009), as well as in the regulation of gene transcription either by direct interaction with RNA-polymerases (Philimonenko et al., 2004), by chromatin remodeling (Kapoor et al., 2013), or by direct regulation of the activity of transcription factors (Vartiainen et al., 2007).

* Corresponding authors.
Email addresses: ralbalat@ub.edu (R. Albalat); canestro@ub.edu (C. Cañestro)
[1] Author equal contribution.

https://doi.org/10.1016/j.ydbio.2018.09.003
Received 30 May 2018; Received in revised form 13 July 2018; Accepted 5 September 2018
Available online xxx

One of the most dramatic specializations that cytoskeleton actin filaments have acquired is contractility thanks to the recruitment of myosin II motor proteins (Lodish et al., 2000). Vertebrate striated muscle cells represent the evolution of one of the most sophisticated actomyosin contractile complexes, in which bundles of filaments organized in sarcomeres can contract quickly, repetitively through long distance and with enough force to drive movement (Lodish et al., 2000). The acquisition of contractility by the recruitment of myosin II motors into actin filaments has not only occurred in muscle cells, but other non-muscle cells have also evolved analogous systems (Conti and Adelstein, 2008; Vicente-Manzanares et al., 2009; Zaidel-Bar et al., 2015). For instance, actin filaments and myosin-II assemble into a contractile ring during cytokinesis that provides mechanical forces for cell cleavage at the end of mitosis (Pollard, 2010). Similarly, other ring-like or circumferential belt contractile structures of actomyosin in the inner surface of cell membranes are fundamental for cell-cell adhesion, wound healing and epithelial extrusions (Nakajima and Tanoue, 2012; Schwayer et al., 2016).

Actins are one of the most conserved proteins in eukaryotes, with a 97% conserved sequence identity across distant species such as sea anemone and human. Classically, actins have been classified into muscle actins and cytoplasmic (or non-muscle) actins, depending on whether they were specialized in muscle contraction or, on the contrary, they form part of the cytoskeleton and were involved in many other cellular functions (Hightower and Meagher, 1986; Vandekerckhove and Weber, 1978). In mammals, for instance, from the six major actin genes that have been identified, four are muscle-specific (alpha-skeletal *ACTA1*, alpha-cardiac *ACTC1*, alpha-smooth muscle *ACTA2*, gamma-smooth muscle *ACTG2*), and two are cytoplasmic (beta-cytoplasmic *ACTB* and gamma-cytoplasmic isoactin *ACTG1*) (Vandekerckhove and Weber, 1978). Muscle-specific actin genes have also been described in non-chordate deuterostomes and protostomes (see Hooper and Thuma, 2005 for an extensive review). In *Drosophila melanogaster*, for instance, four out of its six actin genes (*act57A*, *act87E*, *act88F* and *act79B*) are expressed in muscle tissues of different structures during different times of the life cycle (Fyrberg et al., 1983). Recent phylogenetic analysis based on accurate tree-based orthology estimation has shown that despite their conserved muscular expression, chordate and non-chordate muscle actin genes are not orthologous, but they have a polyphyletic origin due to independent duplications from cytoplasmic genes in different lineages (Inoue and Satoh, 2018). This finding is consistent with previous analyses that based on comparisons of diagnostic positions and exon-intron structures had classified muscle-specific genes of non-chordate animals together with the cytoplasmic actin genes (Chiba et al., 2003; Fyrberg et al., 1981; T. Kusakabe et al., 1997; Vandekerckhove and Weber, 1984).

In cephalochordates, in addition to muscle and cytoplasmic actins, a third group has been described as notochord-type actin genes (N-actin) because of their specific expression in the notochord (Suzuki and Satoh, 2000). The notochord of amphioxus has the peculiarity to be formed by muscle fibers, which in 1870, Muller already described as arranged birefringent myofilaments capable of contracting and altering its mechanical properties upon nervous stimulation (Flood et al., 1969; Müller, 1870). Large scale analysis of notochord ESTs revealed indeed that 11% of its cDNAs was related to muscle genes –including N-actin and many other muscle genes such as tropomyosin, troponin I, myosin regulatory light and heavy chains (Suzuki and Satoh, 2000). The study of the actin gene family has become useful to investigate the origin and evolution of the notochord and the paraxial muscle, and thus, to better understand the origin of the fish-like ancestral chordate body plan that probably was characterized by its swimming capability powered by tail beating (Satoh, 2016). In this work, we focus on the characterization of actin gene family in the appendicularian *Oikopleura dioica*. Appendicularians (a.k.a. larvaceans), ascidians and thaliaceans belong to the urochordate phylum (Satoh et al., 2014), which is the sister group of vertebrates, and together with cephalochordates constitute the chordate superphylum. Appendicularians, in contrast to other urochordates, do not suffer a drastic metamorphosis and maintain their body plan, including an actively motile tail that confers them a free-living pelagic style during their entire life cycle (Mikhaleva et al., 2015; Nishida, 2008; Soviknes et al., 2007; Soviknes and Glover, 2008). Our work reveals how muscle and cytoplasmic actin genes have undergone extensive gene duplications during the evolution of the appendicularian lineage, and reveals cardio-paraxial and notochord-specific expression domains of some muscular and cytoplasmic actin genes that help to better understand the role of actins during the origin and evolution of chordates.

2. Material and methods

2.1. Biological material

O. dioica specimens were obtained from the Mediterranean coast of Barcelona (Catalonia, Spain), and cultured in our animal facility at the University of Barcelona, in which embryos have been collected as described (Marti-Solans et al., 2015).

2.2. Genome survey, phylogenetic analysis, Diagnostic-Actin-Value (DAV) and exon-intron organization

To identify *O. dioica* actin homologs, we made BLAST searches (Altschul et al., 1997) in the genome database of *O. dioica* (Oikobase, http://oikoarrays.biology.uiowa.edu/Oiko) using as queries known actin sequences from ascidians, amphioxus and two cDNAs described in *Oikopleura longicauda* (Nishino et al., 2000). Gene annotations were manually corrected using ESTs and sequences from PCR fragments we have cloned during our analyses.

Phylogenetic trees were made by maximum-likelihood inferences calculated with PhyML v3.0 using automatic Akaike Information Criterion for the substitution model and aLRt SH-like for branch support (Lefort et al., 2017), and by Bayesian inferences calculated by MrBayes 3.2.6 using invgamma model for among-site rate variation, WAG amino acid rate matrix, 2 million generations, in two parallel runs sampling every 1000 generations, and discarding 0.25 of sampled values as burnin to calculate branch support for posterior probabilities (Ronquist et al., 2012).

To analyze the muscular or cytoplasmic nature of actin genes, we have developed an algorithm that calculates the "Diagnostic-Actin-Value" (DAV) according to the conservation of previously described diagnostic positions (Nishino et al., 2000; Vandekerckhove and Weber, 1984) (for details see Sup. File 1). Briefly, according to the classification as muscular or cytoplasmic actins in the phylogenetic tree (branching support = 0.98), first we calculated the frequency of residue conservation of each diagnostic position among all 95 analyzed actins of vertebrates and ascidians. Then, to calculate the DAV, each position contributed with +1 or -1 if the residue was conserved in at least 20% of the muscular or cytoplasmic sequences, respectively. In case that a conserved residue for a group of actins was also found in sequences of the other group, the absolute value of the contribution for each position (i.e. +1 or -1) was corrected by subtracting the frequency of that residue in the other group. According to this algorithm, DAV can range from +16 to -16 depending on the total conservation of muscular or cytoplasmic diagnostic positions, respectively.

To analyze the exon-intron structure of actin genes we used the software GECA (Fawal et al., 2012), defining at least 70% of similarity in the 20 amino acids surrounding the intron position.

2.3. Cloning and expression analysis

Probes for whole-mount in situ hybridization (WMISH) of *O. dioica* actins were PCR amplified and cloned with the Topo TA Cloning® Kit of Invitrogen (primers are listed in Sup. File 2 Table S1). Probes were designed on the 3′ untranslated regions in order to avoid cross-hybridization among paralogs. Cloning, sequencing, and WMISH experiments on fixed embryos at selected developmental stages were performed as previously described (Marti-Solans et al., 2015).

2.4. Nuclear and phalloidin staining

For nuclear and phalloidin staining, embryos were fixed in 4% paraformaldehyde in fixation buffer (0.1 M MOPS, 0.5 M NaCl, 2 mM MgSO4, 1 mM EGTA). After 1 h at room temperature, fixation buffer was replaced by washing twice in PBST (PBS Tween-20, 0,2%). Phalloidin and nuclei stainings were performed incubating the embryos in staining solution (1 μM Hoeschst-33342 Invitrogen-62249, 0.1 μM TRITC-Phalloidin Sigma-P-1951 in PBST) for 1 h at 37 °C in the dark. Stained embryos were washed in PBST and mounted in glycerol 80% in PBS, and photographed in a Fluorescent microscope (Zeiss Aixophot).

3. Results

3.1. Characterization and evolutionary history of Oikopleura dioica actin genes

Our survey of genomic and transcriptomic databases of *O. dioica* identified seven actin genes (labeled in red in Fig. 1**A and** Sup. Fig. S1) distributed in six scaffolds, whose annotations were manually curated and fixed according to available ESTs and our PCR clones (Sup. File 2 Table S2). Phylogenetic analysis suggested that four *O. dioica* actin genes were homologs to chordate muscle actin genes (namely *ActnM1*, *ActnM2*, *ActnM3* and *ActnM4*), whereas the other three grouped with the cytoplasmic ones (*ActnC1*, *ActnC2* and *ActnC3*). The fact that all *O. dioica* ActnM grouped in a single cluster together with a cDNA actin previously described in *Oikopleura longicauda* (Nishino et al., 2000), but without including any muscular actin from other urochordate species, suggested that *ActnMs* of *O. dioica* were paralogs that have been originated by independent gene duplications during the evolution of appendicularians, after their split from ascidians. Cytoplasmic *ActnC* genes of *O. dioca*, on the other side, grouped in two different clusters with moderate support (i.e. 0.91 and 0.88), one including *ActnC1* and *ActnC2*, and the other *ActnC3* (red circles in Fig. 1**A**). The fact that these two clusters also included actins from phlebobranchia and stolidobranchia ascidian species (dark and light blue circles, respectively, in Fig. 1**A**) suggested that their origin might come from ancient duplications that occurred at least before the split of the appendicularian and the ascidian lineages, followed by further duplications in the appendicularian lineage that gave rise to *ActnC1* and *ActnC2*.

Amino-acid sequence identity within the muscular and cytoplasmic actins of *O. dioica* was high, being > 99.5% among ActnMs and > 95% among ActnCs (Sup. File 2 Table S2). The fact that ActnM2 and ActnM3 were identical, and that the other *O. dioica* ActnMs did not differ in more than two amino acids was compatible with either the possibility that duplications that originated these paralogs were recent, or that all ActnM sequences were so similar because they have shared high functional redundancy and have been evolving under the same selective restrictions. Among cytoplasmic actins, ActnC1 and ActnC2 differed in 4 amino acids, while ActnC3 was the most divergent, showing up to 18 amino acid differences. Comparison between *O. dioica* muscle and cytoplasmic actins revealed that their lengths differed in 6 amino acids, due to a 18 nucleotides expansion of the first exon in the muscle actins during the evolution of the *O. dioica* lineage, absent in *O. longicauda*. *O. dioica* muscle and cytoplasmic actins showed 28–33 amino acid differences, suggesting differential selective restrictions for sequence variability between the two groups.

The high sequence similarity among *O. dioica* actins prompted us to analyze their exon-intron structures to look for further support that they were different genes rather than allelic variants. Differences in the exon-intron structures (Sup. File 2 Fig. S2), together with the lack of sequence similarity between introns or untranslated regions (Sup. File 2 Table S3), discarded the possibility that the small number of amino acid differences among genes could be polymorphic variants, and corroborated therefore that the actin catalogue in *O. dioica* is made of seven genes. The exon-intron organization of most *O. dioica* actin genes was, indeed, considerably divergent from the structure that is broadly conserved in actin genes of other species (Sup. File 2 Fig. S2), which was consistent with the high intron turnover described for most genes in *O. dioica* (Edvardsen et al., 2004). Interestingly, the four muscle actin genes (*ActnM1–4*) shared a synapomorphic intron 1, absent in cytoplasmic actins, which corroborated their paralogy and that all *ActnM* genes originated by gene duplication during the appendicularian evolution (intron 1 in red Sup. File 2 Fig. S2). Likewise, the presence of at least two introns in *O. dioica ActnC1* and *ActnC2* that were synapomorphically conserved in other chordate cytoplasmic actin genes supported their position in the phylogenetic tree. The absence of introns in *ActnC3* could be explained either by events of intron loss, a common phenomena observed in many *O. dioica* genes (Denoeud et al., 2010), or by an evolutionary origin related to retrotranscription and integration of a transcript from an ancestral *ActnC* gene. The presence of an intron in *ActnM1* in the same position that in the *ActnC* genes prompted us to analyze the possibility of gene conversion by unequal crossing-over between the two groups of actins. Comparisons of the sequences of the intron and surrounding exons, however, revealed no evidence of gene conversion, concluding that the origin of that intron in *ActnM1* might be due to a convergent intron gain, a phenomenon also observed in several *O. dioica* genes (Denoeud et al., 2010).

To further corroborate the muscular and cytoplasmic nature of *O. dioica ActnM* and *ActnC* genes, we also analyzed the diagnostic positions that had been previously described to differentiate muscle and cytoplasmic actins (Vandekerckhove and Weber, 1984). To perform this analysis, we developed a novel algorithm that calculates the "Diagnostic-Actin-Value" (DAV) according to the conservation of diagnostic positions across an extended list of vertebrates and urochordate actins, adopting more positive or negative values, between + 16 and -16, according to the more muscle or more cytoplasmic characteristics of their sequences, respectively (Sup. File 1). In *O. dioica*, all muscular ActnM shared a DAV of +15.38, while the cytoplasmic actins ActnC1 and ActnC2 had a DAV of -15.42, and ActnC of -9.1 (Fig. 1**B**). These values strongly supported the assignment of their muscle or cytoplasmic nature reflected in the phylogenetic tree (Fig. 1**A**).

Results from our phylogenetic analysis, in which we included new actins from a broad panel of ascidian species, corroborated previous work showing how muscle actins experienced a gene duplication that originated two paralogous groups during the evolution of ascidians, classically referred as "larval" and "adult body-wall" ascidian actins (reviewed in Kusakabe, 1997), and recently renamed as ascidian-P (for Paraxial) or ascidian-B (for Body-wall) actins, respectively (Inoue and Satoh, 2018). However, none of our phylogenetic analyses, neither using maximum likelihood nor Bayesian approaches, unfortunately, provided robust support to clarify the relationship between *O. dioica* and ascidian-P and -B groups, in many cases collapsing in a trichotomy (Fig. 1**A** and Sup. File 2 Fig. S3). Interestingly, the DAV of all *O. dioica ActnM* paralogs (average 15.38) was closer to those of ascidian-P actins (average 14.69 ± 0.78) than those of ascidian-B actins (average of 12.41 ± 0.56), suggesting therefore that *O. dioica* ActnMs had a closer

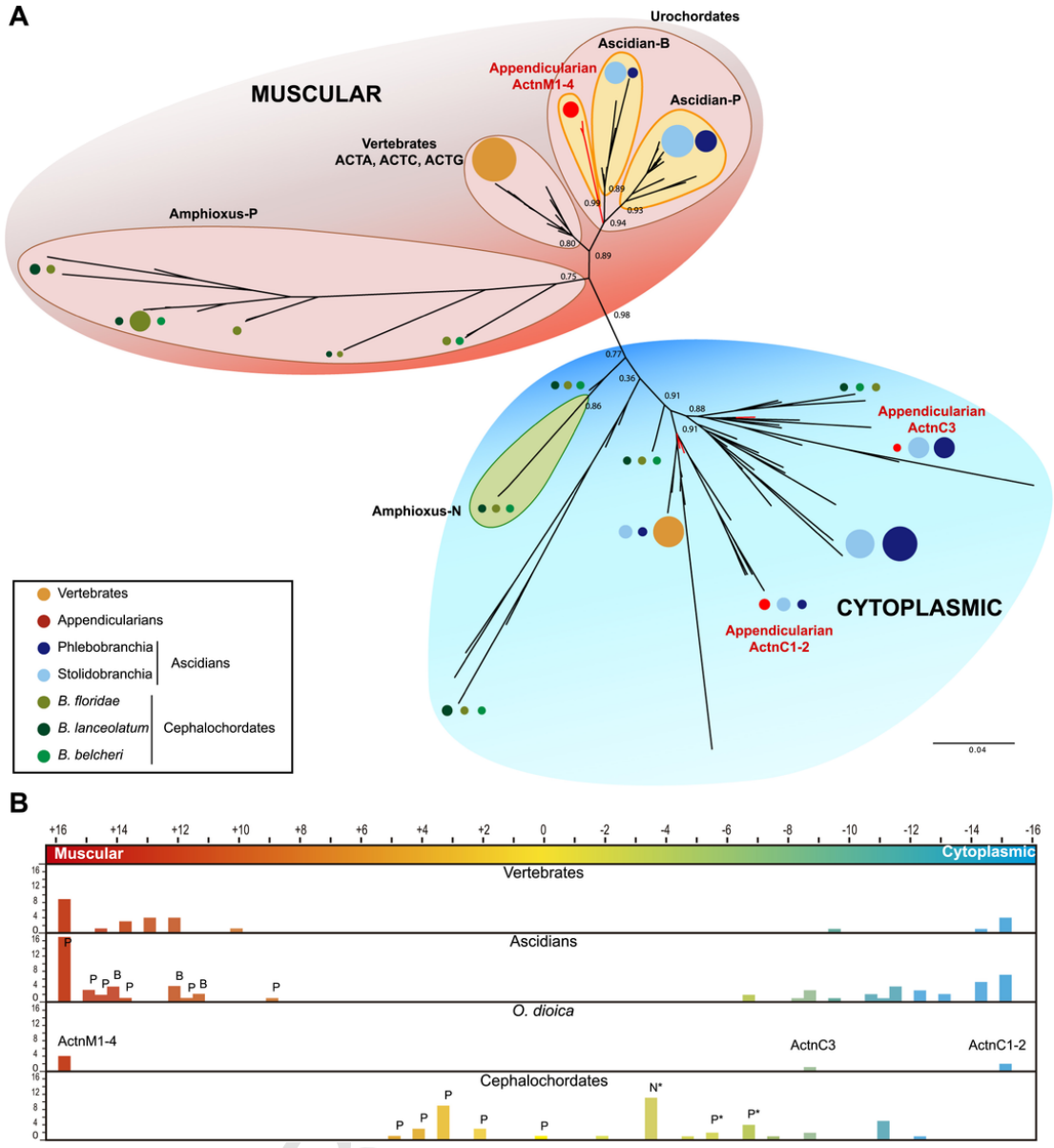

Fig. 1. Evolutionary history and analysis of diagnostic positions of muscular and cytoplasmic actins in chordates. (A) Phylogenetic tree inferred by maximum-likelihood of muscular (in red background) and cytoplasmic (in blue background) actins in chordates. Appendicularian ActnM1–4 and ActnC1–3 are labeled in red. For the sake of clarity, sequence species are depicted as circles with sizes proportional to the number of represented sequences and color coded according to species taxonomy as indicated in the legend (vertebrates in ochre, cephalochordate species in three different green tones, Phlebobranchia and Stolidobranchia ascidians in dark and light blue tones, respectively). Major actin groups are indicated, and values for the approximate likelihood-ratio test (aLRT) are shown in main nodes. Scale bar indicates amino acid substitutions. Fully detailed tree with all sequence names and branch supports are provided in Sup. File 2 Fig. S1. **(B)** Gradient colored representation from totally muscular (+16 in red) to totally cytoplasmic (-16 in blue) DAVs (Diagnostic-Actin-Values) of vertebrate, ascidian, *O. dioica*, and cephalochordate actins. Bars represent the number of sequences (y-axis) included in DAV ranges (x-axis on top). *O. dioica* ActnMs and ActnCs, ascidian-P and -B actins, and amphioxus-P and -N actins are labeled on top of the bars. Asterisks indicate that in addition to -P or -N actins, other cytoplasmic actins having the same DAV are included in the bar.

structural and likely functional relationship to ascidian-P actins than to ascidian-B actins (Fig. 1**B**). Further sequencing of actin genes in additional urochordate groups, especially in doliolids and salps as well as in other appendicularian species, will be necessary to solve the evolution of muscle actin genes in urochordates, and to clarify whether the duplication that gave rise to the P and B paralogs occurred before or after the appendicularian-ascidian split.

3.2. Developmental expression atlas of Oikopleura dioica actin genes

In order to create a detailed developmental atlas of actin expression in *O. dioica*, we investigated the expression patterns of the seven actin genes by whole mount in situ hybridization (WMISH) throughout eight developmental stages from egg to late hatchling (Fig. 2**A-BD**). The high sequence similarity among the seven actin genes, however, hampered these analyses since we noticed that probes designed in coding regions could cross-hybridize among different actins (Sup. File 2 Table S2). To avoid cross-hybridization, therefore, we were forced to design all actin probes in regions of the 3′ untranslated regions that showed lower similarity to other actin genes (Sup. File 2 Table S3), which in some cases rendered small probes (< 100 bp) that required long staining periods up to three weeks in order to detect the signal.

WMISH results revealed that *ActnM* genes had tissue specific expression, which consistent with their 'phylogenetic' muscular nature

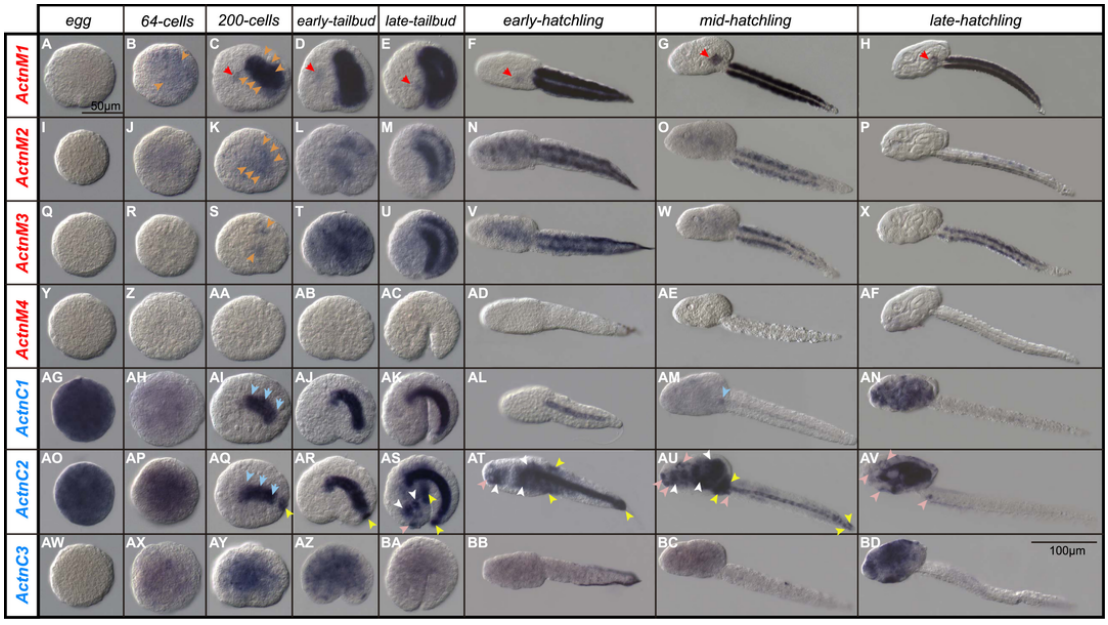

Fig. 2. Expression atlas of muscular and cytoplasmic actins during *Oikopleura dioica* development. Developmental (columns from egg to late-hatchling stage,) expression analysis by whole-mount in situ hybridization of *O. dioica* muscular (**A-H**, *ActnM1*; **I-P**, *ActnM2*; **Q-X**, *ActnM3*; **Y-AF**, *ActnM4*) and cytoplasmic (**AG-AN**, *ActnC1*; **AO-AV**, *ActnC2*; **AW-BD**, *ActnC3*) actin paralogs. Arrowheads: heart (red), paraxial muscle (orange), notochord (blue), epidermis (yellow), nervous system (pink), endoderm (white). Scale bars for eggs to late-tailbud (**A**, 50 µm), from early- to late-hatchling (**BD**, 100 µm).

appeared to be restricted to the muscle cell lineage (Fig. 2**A-AF**). Despite *ActnM* paralogs showed important overlap in their expression domains, they also displayed noticeable dissimilarities that suggested differences in their spatio-temporal regulation, confirming the specificity of the probes used in our WMISH experiments. Temporal differences were shown, for instance, by the time of the expression onset, in which *ActnM1* signal was the earliest to be observed by the 64-cell stage (Fig. 2**B**), followed by *ActnM2* and *ActnM3*, which did not show obvious signal up until the 200-cell stage and early-tailbud stage, respectively, in all cases labeling paraxial muscle cells (Fig. 2**K, S, T,** orange arrowheads). From the late tail-bud up to mid-hatchling stage, the signal of *ActnM1*, *ActnM2*, and *ActnM3* remained constant. By late hatchling stage, however, *ActnM2* seemed to downregulate as its expression signal appeared to be fainter (Fig. 2**P**). Spatial differences in the expression of *ActnM* genes were shown by *ActnM1*, which besides paraxial muscle, it was also expressed in the cardiac cell lineage (Fig. 2**C-H**). We did not observe any signal of *ActnM4* in any of the many WMISH experiments we performed, not even decreasing the stringency of the conditions of the hybridization nor after long staining periods. It is possible that *ActnM4* might be expressed during adult stages, although we cannot discard that the limited small size of the specific probe of this paralog (i.e. 96 nucleotides) might be hampering the detection of signal, especially if this gene was lowly expressed during development in comparison with the other *ActnM* paralogs.

In the case of cytoplasmic genes (Fig. 2**AG-BD**), only one of the three paralogs, namely *ActnC3*, showed a generalized broad expression pattern after long staining periods. The expression of this gene therefore, could be consistent with a basic housekeeping function, which is expected from ubiquitously expressed cytoplasmic actins related to components of the cytoskeleton **(**Fig. 2**AX-BD**). However, the other two *ActnC* paralogs, namely *ActnC1* and *ActnC2*, showed highly dynamic tissue-specific expression patterns changing over time in different organs **(**Fig. 2**AG-AV**). Thus, unfertilized eggs displayed strong signal for *ActnC1* and *ActnC2*, suggesting that these two paralogs were maternally transcribed (Fig. 2**AG, AO**). By the 64-cell stage, most cells still showed *ActnC1* and *ActnC2* signal, but weaker than in eggs, suggesting that it likely was part of the still remaining maternal component (Fig. 2**AH, AP**). By the 200-cell stage, while the maternal signal of *ActnC1* and *ActnC2* was not detected anymore, the entire notochord appeared obviously stained by both paralogs, suggesting that the first zygotic expression of these two paralogs was notochord specific (Fig. 2**AI, AQ** blue arrowheads). This strong signal remained in the notochord throughout tailbud and early-hatchling stages, but in mid-hatchlings, while *ActnC2* signal was still obvious in the entire notochord, *ActnC1* signal appeared to have fainted in most of the notochord except in the first most rostral cell (Fig. 2**AM** blue arrowhead). By the 200-cell stage, in addition to the notochord, the *ActnC2* expression signal was also detected in an ectodermal domain restricted to the most distal cells of the tail, corresponding to the developing tailbud region (Fig. 2**AI, AQ** yellow arrowhead). This *ActnC2* expression domain in the tailbud remained strongly labeled during tailbud and hatchling stages, but disappeared by late-hatchling stage coinciding with the time at which the tail stops elongating (Fig. 2**AV**). By the late-tailbud stage, *ActnC2* signal showed a new expression domain broadly extended in the trunk, including endodermal-, neural- and epidermal-derived tissues, which remained throughout all analyzed hatchling stages (Fig. 2**AS-AV** white, pink and yellow arrowheads for endodermal, neural and epidermal domains, respectively; for details see below next result section). By the late-hatchling stage, in addition to *ActnC2,* the expression signal of *ActnC1* and *ActnC3* also appeared for the first time throughout the trunk (Fig. 2**AN, BD**).

Overall, the developmental atlas of actin expression revealed that both muscle and cytoplasmic actin genes have gone through a complex process of sub-functionalization and/or neofunctionalization after extensive gene duplications during the evolution of appendicularians, in which different paralogs would have acquired notorious differences in their spatio-temporal regulation.

3.3. Detection of actin filaments during Oikopleura dioica development

To visualize actin filaments we used phalloidin staining. While in stages prior to tailbud phalloidin stained most cells (data not shown), by tailbud stage, phalloidin signal was specially obvious in the membranes of notochordal cells, as well as in the membranes of internal

cells of the trunk, the internal part of the trunk-tail junction, and in a very restricted area in the most distal part of the tail corresponding to the tailbud (Fig. 3**A**). Most regions that were stained for phalloidin recapitulated the observed expression domains of *ActnC1* and *ActnC2* (Fig. 3**B and** Fig. 2**AG-AV**). Muscle cells at tailbud stage, however, despite the strong expression of three *ActnM* paralogs (namely *ActnM1*, *M2* and *M3*), did not show any phalloidin staining, suggesting therefore that actin had not polymerized yet, and myofilaments had not been formed at this developmental stage (Fig. 3**C,D**).

After hatching, phalloidin staining revealed the typical "striated" organization of actin myofilaments of the skeletal muscle throughout the tail (Fig. 3**E-G**). The fact that the tail switches 90° respect to the trunk during *O. dioica* development (Cañestro et al., 2005) makes the muscle cells lie in the dorsal and ventral sides of the tail. Thus, from a ventral view, phalloidin-labeled myofilaments displayed a striated pattern spanning the width of the notochord (Fig. 3**E**), whereas from a lateral view, they appeared as two dense lines close to the membrane near the notochord **(**Fig. 3**G)**. In late hatchling stages, phalloidin staining revealed dark and bright bands of the striated pattern corresponding to the presence of sarcomeres in the paraxial muscle in the tail, as well as a clear dark demarcation corresponding to the border of muscle cells (Fig. 3**K**). The actin of myofilaments likely corresponded to the products of *ActnM* paralogs **(**Fig. 2**)**.

In late hatchlings, in addition to the broad phalloidin signal labeling most of the cytoskeleton attached to cell membranes, we observed strong signal in different parts of the digestive system (i.e. the mid-dorsal part of the endostyle, the floor and roof of the esophagus, the internal membranes of stomach lobules, the rectum and the ciliary rings within the gills), the nervous system (i.e. rostral paired nerves n1, the sensory vesicle, the ciliary funnel, the ventral organ and some cells in the anterior third of the caudal ganglion), as well as the base of the placode derived structures of the Langerhans receptors (Fig. 3**G-K**). All these rich actin domains expressed *ActnC2*, and all of them have in common either the presence of cilia (Fig. 3**K**) or axonal projections.

4. Discussion

The present study identifies the complete catalogue of actin genes in *O. dioica*, which based on phylogenetic analyses, intron positions, DAVs and expression patterns is made of four muscular *ActnM1–4* and three cytoplasmic *ActnC1–3* genes. Our work also suggests that the multiple paralogs that belong to each group of actins have been mostly originated by lineage-specific duplications during the evolution of the appendicularians. Our results corroborate the muscular and cytoplasmic homologies assigned to two actin cDNAs that had previously been isolated in *O. longicauda* (Nishino et al., 2000), as well as to six *O.*

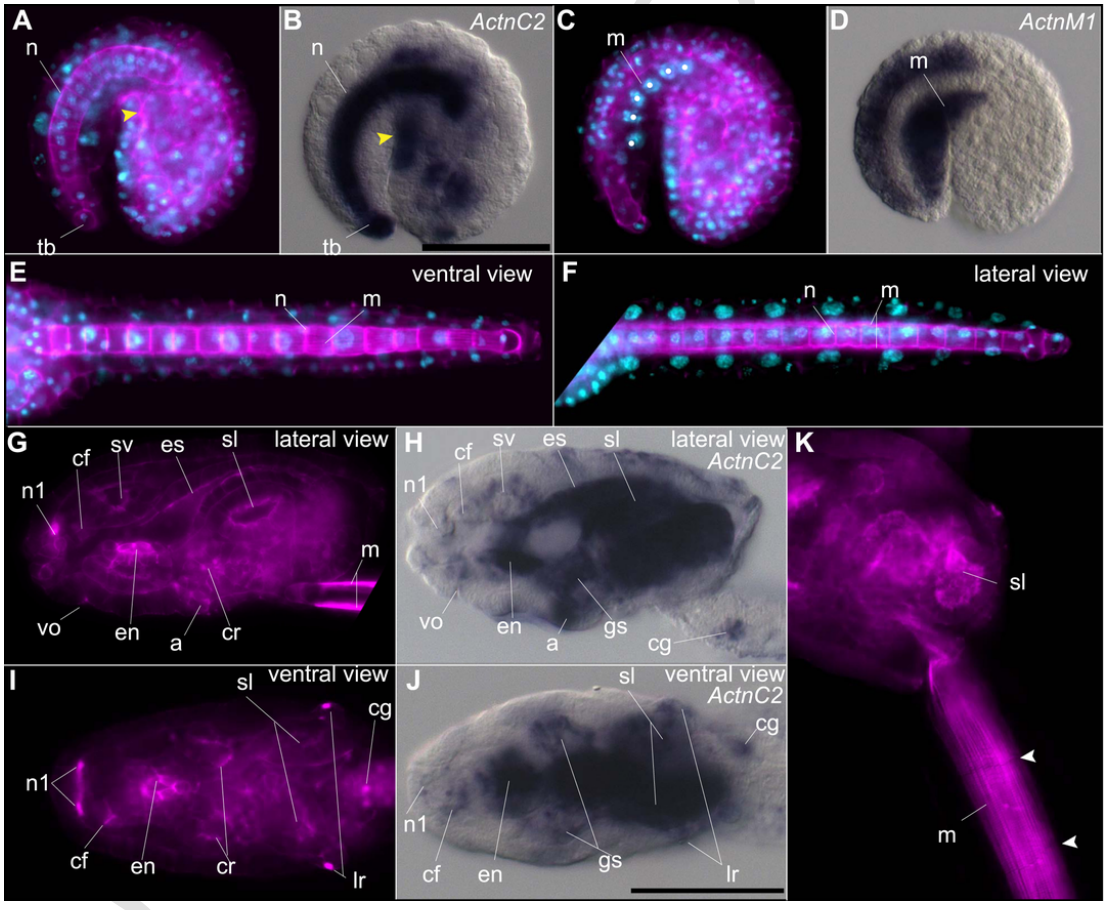

Fig. 3. Correlation between actin-filament detection by phalloidin-staining and actin paralog gene expression. (A-D) At tailbud stage (lateral views), phalloidin staining (**A**, **C**, magenta) labeled cells in the trunk, specially of the internal membrane of the epidermal cells and the cells in the internal area of the trunk-tail junction (yellow arrowhead), notochord (n) and the tailbud (tb), consistently with *ActnC2* expression **(B)**, but it did not label muscle (m) cells (white dots on Hoeschst-stained nuclei in blue) despite the strong expression of *ActnM* genes **(D). (E-F)** After hatching, however, phalloidin-stained myofilaments in muscle cells could be observed from a ventral view displaying a striated pattern **(E)**, and forming two lines near the notochord from a lateral view **(F)**. **(G-J)** In late hatchling stages, phalloidin labeled endodermal tissues such the endostyle (en), esophagus (es), stomach lobes (sl), the ciliary rings in the gills (gs) and anus (a), neural derivatives such as the paired nerves 1 (n1), ciliary funnel (cf), sensory vesicle (sv), ventral organ (vo), caudal ganglion (cg), and the placode derived Langerhans receptors (lr). The presence of actin in these organs was consistent with the expression of *ActnC2*. All these structures had in common either the presence of cilia or axonal projections. In tail shift stage **(K)**, phalloidin-stained cilia were easily observed within the stomach lobe. At this stage, phalloidin staining also revealed the presence of dark and light bands typical of sarcomeres of the striated muscle, and it also labeled the limits of each muscle cell (white arrowheads).

dioica actins predicted by an automatic orthology pipeline designed to identify muscle genes in deuterostome genomes (Inoue and Satoh, 2018). Previous analyses of ascidian actins (Beach and Jeffery, 1990; Chiba et al., 2003; Kovilur et al., 1993; Kusakabe et al., 1995, 1992, 1996; Swalla et al., 1994; Tomlinson et al., 1987) together with our genomic survey and phylogenetic analyses suggest that different ascidian lineages seem to have also expanded their actin catalogues independently (i.e. at least 14 in *Ciona robusta* –formerly *C. intestinalis*–, 9 in *Ciona savignyi*, 16 in *Phallusia mammillata*, 8 in *Molgula oculata*, 9 in *Molgula occidentalis*, 16 in *Halocynthia roretzi*, and 11 in *Botryllus schlosseri*) (Sup. File 2 Fig. S2 and S3).

4.1. Ancestral "cardio-paraxial" muscular actin in stem olfactores

In the case of ascidian muscle actins, our phylogenetic study shows that ascidian-P and -B paralogous groups are present in all ascidian species analyzed in both Phlebobranchia and Stolidobranchia orders. This fact reinforces results from previous work that had suggested that the origin of these paralogous groups was due to an ancient gene duplication that occurred during early ascidian evolution (Inoue and Satoh, 2018). Unfortunately, current available sequences do not contain enough phylogenetic signal to provide robust enough support to determine if that duplication occurred before or after the appendicularian-ascidian split. Our findings, however, favor the scenario that the duplication occurred after the appendicularian-ascidian split because *O. dioica* ActnMs seem to share a mix of characteristics with both ascidian-P and -B groups, which may represent the ancestral urochordate condition. On one side, the DAVs of *O. dioica* ActnMs are closer to those of ascidian-P than to those of ascidian-B actins. The sequence resemblance with ascidian-P may be due to similar molecular interactions with specific actin-binding proteins of the myosin motor machinery (Perrin and Ervasti, 2010), which are necessary to drive tail movement in both *O. dioica* and ascidian larvae. On the other side, the expression pattern of *O. dioica ActnM1* shares expression domains with ascidian-P and -B in paraxial muscle and heart (see a summary of *C. robusta* actin expression data Sup. File 2 Fig. S4 from ANISEED (www.aniseed.cnrs.fr); although cross-hybridization between probes of ascidian-P and -B actin genes, which share an overall 87% of identity, cannot be discarded (Brozovic et al., 2018)). Our results, therefore, are consistent with an evolutionary scenario in which stem urochordates had an ancestral "cardio-paraxial" actin gene that was involved both in heart and paraxial muscle development (Fig. 4). Then, in agreement with recent work by Inoue and Satoh (Inoue and Satoh, 2018), after the split between the appendicularian and ascidian lineages, the ancestral "cardio-paraxial" actin was duplicated in ascidians, experiencing a process of subfunctionalization in which ascidian-P actins mostly evolved under selective restrictions related to motor-tail movement, and ascidian-B actins mostly evolved under the selection of post-metamorphic innovations, such as adult body-wall muscle and adult heart slow paced contractility (Fig. 1**B**). Studies of further actins in additional urochordate groups, especially in doliolids and salps and other appendicularians species, will be necessary to corroborate or disprove this hypothesis. To our knowledge, appendicularians do not have any tissue homologous to the body-wall muscle present in ascidians or some thaliaceans, so further studies of the phylogeny and expression of actins from these different groups will possibly help to better understand the origin and evolution of body-wall muscle in urochordates (Degasperi et al., 2009).

Analyses in vertebrates had hypothesized that the last common ancestor of vertebrates also had an actin that was expressed both in paraxial muscle and heart (Vandekerckhove and Weber, 1984). Our work comparing urochordates and vertebrates points to an older origin of the "cardio-paraxial" actin present at least in the last common ancestor of olfactores (urochordates + vertebrates), since *ActnM1* in *O. dioica,* the ascidian-B *Ci-Ma2* in *C. robusta*, and the alpha-cardiac *ACTC1* and the alpha-skeletal *ACTA1* in vertebrates share expression in both cardiac and paraxial muscle cell precursors during embryo development (Fig. 4) (Mayer et al., 1984; Ordahl, 1986; Schwartz et al., 1986). While *ActnM1* seems to be the only *ActnM* paralog expressed during heart development in *O. dioica,* in vertebrates, three alpha muscle actins are sequentially expressed during cardiac development. *ACTA2* expression starts marking the onset of cardiomyocyte differentiation, which is sequentially replaced first by *ACTA1* and later by *ACTC1*. This process has been related to the regulation of the specific functional activities of each actin isoforms in different developmental stages (Bertola et al., 2008; Ruzicka and Schwartz, 1988; Woodcock-Mitchell et al., 1988). During skeletal muscle development, sequential expression of different actins is also observed in vertebrates and *O. dioica*. First *ACTC1* and next *ACTA1* are expressed in vertebrates (Mayer et al., 1984; Schwartz et al., 1986), and *ActnM1* expression is followed by *ActnM2* and *ActnM3* in *O. dioica*. Altogether, our work highlights similarities as well as differences in the parallel evolution that actin paralogs have experienced after being independently duplicated in both urochordates and vertebrates, including subfunctionaliza-

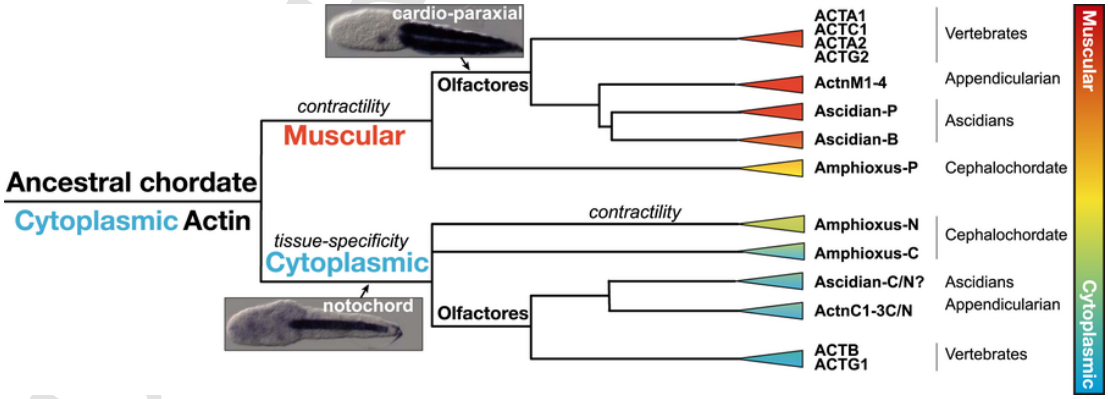

Fig. 4. Schematic representation of the actin evolution in chordates. Muscular actins were originated by an ancestral duplication from a cytoplasmic gene at the base of the chordate superphylum, followed by the acquisition of contractility by the recruitment of the myosin motor-machinery in muscle cells. The ancestral muscle actin of olfactores already played "cardio-paraxial" roles, as currently reflected by *ActnM1* in *O. dioica*. Extensive gene duplications independently expanded muscular actins in vertebrates, appendicularians and ascidians, in the latter originating two paralogous groups, ascidian-P and -B actins. Cytoplasmic actins in chordates show tissue-specific expression patterns, challenging the housekeeping notion classically ascribed to these cytoplasmic (C) actins. Interestingly, our results showing notochord-specific cytoplasmic actins in *O. dioica* likely represents the ancestral condition of chordates. During the evolution of cephalochordates, the recruitment of the myosin motor-machinery to the ancestral cytoplasmic-N actins led also to the acquisition of contractility of the notochord in this lineage. DAV analysis likely reflects the different selective restrictions that apply to the evolution of diagnostic positions according to protein-protein interactions of each group of actins (color code is labeled as in Fig. 1**B).**

tion leading to temporal regulation (i.e. differential expression onsets) and tissue specificity (i.e. paraxial vs cardiac) specializations.

Our phylogenetic analysis corroborates that muscular actins were originated by a gene duplication from an cytoplasmic actin at the base of chordates, before the split between cephalochordates and olfactores, which was followed by the recruitment of the myosin motor-machinery that conferred contractile capability to muscle cells (Inoue and Satoh, 2018). During the evolution of cephalochordates, muscular actins followed complex and divergent evolutionary histories as proposed by previous works describing lineage-specific duplications and events of gene conversion in cephalochordates (Fig. 1**A**) (Inoue and Satoh, 2018; R. Kusakabe et al., 1997a, 1999; Suzuki and Satoh, 2000). Our analysis of DAVs supports a distinctive evolutionary pattern of cephalochordate actins in which none of the muscular actins of amphioxus shows the characteristic high positive values of muscle actins in olfactores **(**Fig. 1**B and** Sup. File 1**)**, but they have lower positive DAVs close to a "neutral" region, in which actins likely share characteristics of both muscular and cytoplasmic actins (Fig. 1**B**). Overall, our results suggest that the evolutionary restrictions of muscle actins related to interactions with motor actin-binding proteins differ between cephalochordates and olfactores.

4.2. Ancestral notochord-specific cytoplasmic actin in stem chordates

Cephalochordates have a third type of actins, named amphioxus-N (notochord) actins that are expressed in the notochord together with many other motor-proteins that confer contractile capability to the notochord (Fig. 4) (Suzuki and Satoh, 2000; Urano et al., 2003). Our phylogenetic analyses and relatively not too negative DAV results of amphioxus-N actins are compatible with the work by Inoue and Satoh that suggested that these actins originated from a duplication of a cytoplasmic actin gene (Inoue and Satoh, 2018), and likely suffered a convergent selective process towards contractile muscular actins. Considering the notochord-specific expression of amphioxus-N actins, our finding that *O. dioica ActnC1* and *ActnC2* are tissue-specific with a prominent expression in the notochord, allow us to infer that the expression of cytoplasmic actins in the notochord likely represents the ancestral condition already present at least in stem chordates **(**Fig. 4**)**. In ascidians, several studies have shown a fundamental role of actin filaments in notochord convergent extension processes during morphogenesis as well as providing stiffness to notochord structure (Jiang and Smith, 2007; Munro and Odell, 2002a, 2002b). Our results detecting actin filaments in the notochord (Fig. 3) are compatible with a potential conservation of actin functions between *O. dioica* and ascidians. To our knowledge, however, no evidence has been found supporting the expression of muscle genes in the notochord of ascidians or appendicularians (Hotta et al., 2000; Jiang and Smith, 2007; Kugler et al., 2011; Takahashi et al., 1999 an our unpublished data). Our findings, therefore, are consistent with the recently postulated hypothesis by Inoue and Satoh, in which the evolution of the amphioxus-N actin and recruitment of muscle genetic machinery in the notochord of cephalochordates would be an innovation of this lineage (Inoue and Satoh, 2018), whereas the urochordate non-contractile actin-expressing notochord, as it is currently found in *O. dioica*, would reflect the ancestral condition of stem chordates (Fig. 4).

In the last years, the evolutionary origin of the notochord has been a hot topic of discussion (Annona et al., 2015; Brunet et al., 2015; Hejnol and Lowe, 2014), especially after the axochord hypothesis suggesting that the notochord could have evolved by modification of a ventromedian muscle axochord present in stem bilaterians (Lauri et al., 2014). During the characterization of the axochord in different bilaterians, phalloidin staining has shown the presence of actin expression in this structure (Lauri et al., 2014). In the light of our new data showing that the notochord-specific expression of cytoplasmic actins is an ancestral chordate condition, future comparative studies of the regulatory mechanisms of actin expression in the axochord and in the notochord, as well as investigations on whether homologous actins are responsible for the process of midline convergence of both axochord (Lauri et al., 2014) and notochord (Jiang and Smith, 2007) could shed some light on the evolution of the notochord, and therefore in the origin of chordates.

4.3. Tissue-specificity and temporal regulation of cytoplasmic actins related to cilia and axonal projections

The notion that cytoplasmic actins are housekeeping genes with constitutive and ubiquitous expression patterns is an extended idea that lately has been challenged, for instance, by cases in which actin expression has been shown not to be appropriate to normalize RNA or protein quantification (Lin and Redies, 2012; Ruan and Lai, 2007). Our results show that from the three ActnC paralogs of *O. dioica*, only *ActnC3* displays a broad non-tissue specific expression pattern consistent with a housekeeping role. Its ubiquitous expression could be related to its possible retrotranscriptional origin and subsequent insertion in a genomic location driving its transcription in a non-tissue-specific manner. In contrast to *ActnC3*, the other two paralogs *ActnC1* and *ActnC2* show remarkable tissue-specific and temporally-regulated expression patterns, not compatible with housekeeping roles (Figs. 2 and 3). In *O. dioica*, the expression domains of these two *ActnC* paralogs –besides the notochord– correlates with regions characterized by either the presence of cilia or axonal projections, as well as regions with presumptive high cell proliferation. In the endostyle, for instance, the expression domain of *ActnC2* is restricted to the central part of the endostyle (mostly dorsal, but also ventral; Fig. 3**H, J**). This region is characterized by the presence of ciliated cells that project giant cilia that can be easily observed with phalloidin staining towards the corridor of this organ (Fig. 3**G,I)**, in which they wind the food trapping secretions towards the pharynx lumen. In the digestive system, *ActnC2* is highly expressed in the esophagus, left and right stomach lobes, vertical and mid intestine, and rectum, which all of them are characterized by the presence of ciliated cells (Burighel and Brena, 2001)(Fig. 3**G-J**). In the pharyngo-branchial region, the expression domains of *ActnC1* and *ActnC2* also correlates with the presence of cilia in the pharynx and the ciliary rings in the gills, the beating of which induce water circulation from the mouth to the gill slits, or in opposite direction depending on the orientation of the beating (Fig. 3**G-J**). In the epidermis, the expression domains of *ActnC2* correlates with the presence of ciliated sensory cells, including the mechanosensory cells in the circumoral organ, the ventral organ and the mechanoreceptors of the Langerhans cells (Fig. 3**G-J**). These sensory structures have been described to be evolutionary related to placodes, which have been hypothesized to be key innovations for the origin and evolution of sensory organs in olfactores (Bassham and Postlethwait, 2005; Manni et al., 2004). In the nervous system, the expression domains of *ActnC2* correlates with either the presence of cilia (i.e. coronet cells in the sensory vesicle whose cilia touch the statocyte likely related to responses to positional cues such as vibration, acceleration or gravity (Bone, 1998; Olsson, 1975)) or axonal projections, such as those forming the rostral paired nerves n1, nerves innervating the ventral organ or neurons in the caudal ganglia projecting towards the motor system (Bollner et al., 1986; Burighel et al., 2011; Cañestro et al., 2005; Soviknes et al., 2007; Soviknes and Glover, 2007). Interestingly, most of these *ActnC2* expression domains with cilia and axonal projections also express one of the two *Pax2/5/8* paralogs of *O. dioica* (Bassham et al., 2008; Cañestro et al., 2008; Cañestro and Postlethwait, 2007), suggesting a potential role of this transcription factor upstream of *ActnC2* during the development of cilia and axonal projections. Finally, we observe *ActnC2* expression in the most distal part of the tail (Fig. 2**AQ-AU**), a region in which presumably high

cell proliferation and cell differentiation may be occurring related to the process of tail elongation. Our finding of non-ubiquitous expression of *ActnC* genes in *O. dioica* is consistent with the tissue-specificity already described for a cytoplasmic actin gene in the ascidian *Halocynthia roretzi*, which showed prominent expression in mesenchymal cells of the trunk, in epidermal mechanoreceptor cells, neurons, cells with cytoplasmic extensions, as well as faint expression in the notochord (Araki et al., 1996). We can conclude, therefore, that the tissue-specificity of cytoplasmic actin genes is likely an ancestral condition of urochordates.

Overall, our results highlight that during the evolution of chordates, cytoplasmic actins did not simply play housekeeping roles, but they also displayed tissue-specific and temporally-regulated expression patterns during a complex evolutionary history with extensive gene duplications. The role of actins in axon projections and the formation of cilia and flagella seems to be of ancient origin (Quarmby, 2014; Roblodowski and He, 2017). However, the recruitment of cytoplasmic actin genes for the development of ciliated cells present in placode-like sensory organs and pharyngo-branchial structures, the recruitment of cytoplasmic actin genes for the development of the notochord, and the duplication of cytoplasmic genes that gave rise to muscular actins involved in cardio-paraxial development appear as crucial events associated to key evolutionary innovations of the chordate body plan.

Authors' contributions

A.A. carried gene cloning and WMISH experiments. Nuclear and phalloidin stainings were carried out by A.A. and A.F-R. A.F-R. performed gene identifications, phylogenetic analyses, exon-intron analyses, and development of DAV algorithm. A.A. and A.F-R interpreted the data and made the figures. R.A. and C.C. supervised the experiments. C.C. conceptualized the project and wrote the MS with input from A.A., A.F-R. and R.A. All authors commented on the manuscript and agreed to its final version.

Acknowledgements

The authors thank to Dr. Jun Inoue and Prof. Noriyuki Satoh for kindly providing actin sequence alignments from their previous work, to Dr. Marta Riutort for helpful assistance and advice on phylogenetic analyses, to Dr. Vittoria Roncalli and Dr. Adriana Rodríguez-Marí for language revision, and to all team members of the C.C. and R.A. laboratories for assistance with the animal facility and fruitful discussions. C.C. was supported by BFU2016-80601-P and R.A. by BIO2015-67358-C2-1-P grants from Ministerio de Economía y Competitividad (Spain). C.C. and R.A. were also supported by grant 2017-SGR-1665 from Generalitat de Catalunya. A.F-R. was supported by a FPU14/02654 fellowship from Ministerio de Educación Cultura y Deporte.

Appendix A. Supporting information

Supplementary data associated with this article can be found in the online version at doi:10.1016/j.ydbio.2018.09.003.

References

Altschul, S.F., Madden, T.L., Schaffer, A.A., Zhang, J., Zhang, Z., Miller, W., Lipman, D.J., 1997. Gapped BLAST and PSI-BLAST: a new generation of protein database search programs. Nucleic Acids Res. 25, 3389–3402.

Annona, G., Holland, N.D., D'Aniello, S., 2015. Evolution of the notochord. Evodevo 6, 30.

Araki, I., Tagawa, K., Kusakabe, T., Satoh, N., 1996. Predominant expression of a cytoskeletal actin gene in mesenchyme cells during embryogenesis of the ascidian Halocynthia roretzi. Dev. Growth Differ. 38, 401–411.

Avasthi, P., Onishi, M., Karpiak, J., Yamamoto, R., Mackinder, L., Jonikas, M.C., Sale, W.S., Shoichet, B., Pringle, J.R., Marshall, W.F., 2014. Actin is required for IFT regulation in Chlamydomonas reinhardtii. Curr. Biol. 24, 2025–2032.

Bassham, S., Cañestro, C., Postlethwait, J.H., 2008. Evolution of developmental roles of Pax2/5/8 paralogs after independent duplication in urochordate and vertebrate lineages. BMC Biol. 6, 35.

Bassham, S., Postlethwait, J.H., 2005. The evolutionary history of placodes: a molecular genetic investigation of the larvacean urochordate Oikopleura dioica. Development 132, 4259–4272.

Beach, R.L., Jeffery, W.R., 1990. Temporal and spatial expression of a cytoskeletal actin gene in the ascidian Styela clava. Dev. Genet. 11, 2–14.

Bertola, L.D., Ott, E.B., Griepsma, S., Vonk, F.J., Bagowski, C.P., 2008. Developmental expression of the alpha-skeletal actin gene. BMC Evol. Biol. 8, 166.

Besse, F., Ephrussi, A., 2008. Translational control of localized mRNAs: restricting protein synthesis in space and time. Nat. Rev. Mol. Cell Biol. 9, 971–980.

Bezanilla, M., Gladfelter, A.S., Kovar, D.R., Lee, W.L., 2015. Cytoskeletal dynamics: a view from the membrane. J. Cell Biol. 209, 329–337.

Blanchoin, L., Boujemaa-Paterski, R., Sykes, C., Plastino, J., 2014. Actin dynamics, architecture, and mechanics in cell motility. Physiol. Rev. 94, 235–263.

Bollner, T., Holmberg, K., Olsson, R., 1986. A rostral sensory mechanism in Oikopleura dioica (Appendicularia). Acta Zool. 67, 235–241.

Bone, Q., 1998. Nervous system, sense organs, and excitable epithelia. In: Bone, Q. (Ed.), The Biology of Pelagic Tunicates. Oxford University Press, New York, pp. 55–80.

Brozovic, M., Dantec, C., Dardaillon, J., Dauga, D., Faure, E., Gineste, M., Louis, A., Naville, M., Nitta, K.R., Piette, J., Reeves, W., Scornavacca, C., Simion, P., Vincentelli, R., Bellec, M., Aicha, S.B., Fagotto, M., Gueroult-Bellone, M., Haeussler, M., Jacox, E., Lowe, E.K., Mendez, M., Roberge, A., Stolfi, A., Yokomori, R., Brown, C.T., Cambillau, C., Christiaen, L., Delsuc, F., Douzery, E., Dumollard, R., Kusakabe, T., Nakai, K., Nishida, H., Satou, Y., Swalla, B., Veeman, M., Volff, J.N., Lemaire, P., 2018. ANISEED 2017: extending the integrated ascidian database to the exploration and evolutionary comparison of genome-scale datasets. Nucleic Acids Res 46, D718–D725.

Brunet, T., Lauri, A., Arendt, D., 2015. Did the notochord evolve from an ancient axial muscle? The axochord hypothesis. Bioessays 37, 836–850.

Burighel, P., Brena, C., 2001. Gut ultrastructure of the appendicularian Oikopleura dioica (Tunicata). Invertebr. Biol. 120, 278–293.

Burighel, P., Caicci, F., Manni, L., 2011. Hair cells in non-vertebrate models: lower chordates and molluscs. Hear. Res. 273, 14–24.

Cañestro, C., Bassham, S., Postlethwait, J.H., 2005. Development of the central nervous system in the larvacean Oikopleura dioica and the evolution of the chordate brain. Dev. Biol. 285, 298–315.

Cañestro, C., Bassham, S., Postlethwait, J.H., 2008. Evolution of the thyroid: anterior-posterior regionalization of the Oikopleura endostyle revealed by Otx, Pax2/5/8, and Hox1 expression. Dev. Dyn. 237, 1490–1499.

Cañestro, C., Postlethwait, J.H., 2007. Development of a chordate anterior-posterior axis without classical retinoic acid signaling. Dev. Biol. 305, 522–538.

Chang, C.H., Lee, H.H., Lee, C.H., 2017. Substrate properties modulate cell membrane roughness by way of actin filaments. Sci. Rep. 7, 9068.

Chiba, S., Awazu, S., Itoh, M., Chin-Bow, S.T., Satoh, N., Satou, Y., Hastings, K.E., 2003. A genomewide survey of developmentally relevant genes in Ciona intestinalis. IX. Genes Muscle Struct. Proteins Dev. Genes Evol. 213, 291–302.

Conti, M.A., Adelstein, R.S., 2008. Nonmuscle myosin II moves in new directions. J. Cell Sci. 121, 11–18.

Degasperi, V., Gasparini, F., Shimeld, S.M., Sinigaglia, C., Burighel, P., Manni, L., 2009. Muscle differentiation in a colonial ascidian: organisation, gene expression and evolutionary considerations. BMC Dev. Biol. 9, 48.

Denoeud, F., Henriet, S., Mungpakdee, S., Aury, J.M., Da Silva, C., Brinkmann, H., Mikhaleva, J., Olsen, L.C., Jubin, C., Cañestro, C., Bouquet, J.M., Danks, G., Poulain, J., Campsteijn, C., Adamski, M., Cross, I., Yadetie, F., Muffato, M., Louis, A., Butcher, S., Tsagkogeorga, G., Konrad, A., Singh, S., Jensen, M.F., Cong, E.H., Eikeseth-Otteraa, H., Noel, B., Anthouard, V., Porcel, B.M., Kachouri-Lafond, R., Nishino, A., Ugolini, M., Chourrout, P., Nishida, H., Aasland, R., Huzurbazar, S., Westhof, E., Delsuc, F., Lehrach, H., Reinhardt, R., Weissenbach, J., Roy, S.W., Artiguenave, F., Postlethwait, J.H., Manak, J.R., Thompson, E.M., Jaillon, O., Du Pasquier, L., Boudinot, P., Liberles, D.A., Volff, J.N., Philippe, H., Lenhard, B., Roest Crollius, H., Wincker, P., Chourrout, D., 2010. Plasticity of animal genome architecture unmasked by rapid evolution of a pelagic tunicate. Science 330, 1381–1385.

Dominguez, R., Holmes, K.C., 2011. Actin structure and function. Annu. Rev. Biophys. 40, 169–186.

Edvardsen, R.B., Lerat, E., Maeland, A.D., Flat, M., Tewari, R., Jensen, M.F., Lehrach, H., Reinhardt, R., Seo, H.C., Chourrout, D., 2004. Hypervariable and highly divergent intron-exon organizations in the chordate Oikopleura dioica. J. Mol. Evol. 59, 448–457.

Farwell, A.P., Lynch, R.M., Okulicz, W.C., Comi, A.M., Leonard, J.L., 1990. The actin cytoskeleton mediates the hormonally regulated translocation of type II iodothyronine 5'-deiodinase in astrocytes. J. Biol. Chem. 265, 18546–18553.

Fawal, N., Savelli, B., Dunand, C., Mathe, C., 2012. GECA: a fast tool for gene evolution and conservation analysis in eukaryotic protein families. Bioinformatics 28, 1398–1399.

Flood, P.R., Guthrie, D.M., Banks, J.R., 1969. Paramyosin muscle in the notochord of Amphioxus. Nature 221, 87–88.

Fritzsche, M., Erlenkamper, C., Moeendarbary, E., Charras, G., Kruse, K., 2016. Actin kinetics shapes cortical network structure and mechanics. Sci. Adv. 2, e1501337.

Fyrberg, E.A., Bond, B.J., Hershey, N.D., Mixter, K.S., Davidson, N., 1981. The actin genes of Drosophila: protein coding regions are highly conserved but intron positions are not. Cell 24, 107–116.

Fyrberg, E.A., Mahaffey, J.W., Bond, B.J., Davidson, N., 1983. Transcripts of the six Drosophila actin genes accumulate in a stage- and tissue-specific manner. Cell 33, 115–123.

Gunning, P.W., Ghoshdastider, U., Whitaker, S., Popp, D., Robinson, R.C., 2015. The evolution of compositionally and functionally distinct actin filaments. J. Cell Sci. 128, 2009–2019.

Hejnol, A., Lowe, C.J., 2014. Animal evolution: stiff or squishy notochord origins?. Curr. Biol. 24, R1131–R1133.

Heng, Y.W., Koh, C.G., 2010. Actin cytoskeleton dynamics and the cell division cycle. Int. J. Biochem. Cell Biol. 42, 1622–1633.

Hightower, R.C., Meagher, R.B., 1986. The molecular evolution of actin. Genetics 114, 315–332.

Hofmann, W.A., 2009. Cell and molecular biology of nuclear actin. Int. Rev. Cell Mol. Biol. 273, 219–263.

Hooper, S.L., Thuma, J.B., 2005. Invertebrate muscles: muscle specific genes and proteins. Physiol. Rev. 85, 1001–1060.

Hotta, K., Takahashi, H., Asakura, T., Saitoh, B., Takatori, N., Satou, Y., Satoh, N., 2000. Characterization of Brachyury-downstream notochord genes in the Ciona intestinalis embryo. Dev. Biol. 224, 69–80.

Inoue, J., Satoh, N., 2018. Deuterostome genomics: lineage-specific protein expansions that enabled chordate muscle evolution. Mol. Biol. Evol.

Jiang, D., Smith, W.C., 2007. Ascidian notochord morphogenesis. Dev. Dyn. 236, 1748–1757.

Kapoor, P., Chen, M., Winkler, D.D., Luger, K., Shen, X., 2013. Evidence for monomeric actin function in INO80 chromatin remodeling. Nat. Struct. Mol. Biol. 20, 426–432.

Kondrikov, D., Fonseca, F.V., Elms, S., Fulton, D., Black, S.M., Block, E.R., Su, Y., 2010. Beta-actin association with endothelial nitric-oxide synthase modulates nitric oxide and superoxide generation from the enzyme. J. Biol. Chem. 285, 4319–4327.

Kovilur, S., Jacobson, J.W., Beach, R.L., Jeffery, W.R., Tomlinson, C.R., 1993. Evolution of the chordate muscle actin gene. J. Mol. Evol. 36, 361–368.

Kugler, J.E., Kerner, P., Bouquet, J.M., Jiang, D., Di Gregorio, A., 2011. Evolutionary changes in the notochord genetic toolkit: a comparative analysis of notochord genes in the ascidian Ciona and the larvacean Oikopleura. BMC Evol. Biol. 11, 21.

Kusakabe, R., Kusakabe, T., Satoh, N., Holland, N.D., Holland, L.Z., 1997. Differential gene expression and intracellular mRNA localization of amphioxus actin isoforms throughout development: implications for conserved mechanisms of chordate development. Dev. Genes Evol. 207, 203–215.

Kusakabe, R., Satoh, N., Holland, L.Z., Kasakabe, T., 1999. Genomic organization and evolution of actin genes in the amphioxus Branchiostoma belcheri and Branchiostoma floridae. Gene 227, 1–10.

Kusakabe, T., 1997. Ascidian actin genes: developmental regulation of gene expression and molecular evolution. Zool. Sci. 14, 707–718.

Kusakabe, T., Araki, I., Satoh, N., Jeffery, W.R., 1997. Evolution of chordate actin genes: evidence from genomic organization and amino acid sequences. J. Mol. Evol. 44, 289–298.

Kusakabe, T., Hikosaka, A., Satoh, N., 1995. Coexpression and promoter function in two muscle actin gene complexes of different structural organization in the ascidian Halocynthia roretzi. Dev. Biol. 169, 461–472.

Kusakabe, T., Makabe, K.W., Satoh, N., 1992. Tunicate muscle actin genes. Structure and organization as a gene cluster. J. Mol. Biol. 227, 955–960.

Kusakabe, T., Swalla, B.J., Satoh, N., Jeffery, W.R., 1996. Mechanism of an evolutionary change in muscle cell differentiation in ascidians with different modes of development. Dev. Biol. 174, 379–392.

Lauri, A., Brunet, T., Handberg-Thorsager, M., Fischer, A.H., Simakov, O., Steinmetz, P.R., Tomer, R., Keller, P.J., Arendt, D., 2014. Development of the annelid axochord: insights into notochord evolution. Science 345, 1365–1368.

Lefort, V., Longueville, J.E., Gascuel, O., 2017. SMS: smart model selection in PhyML. Mol. Biol. Evol. 34, 2422–2424.

Lin, J., Redies, C., 2012. Histological evidence: housekeeping genes beta-actin and GAPDH are of limited value for normalization of gene expression. Dev. Genes Evol. 222, 369–376.

Lodish, H., Berk, A., Zipursky, S.L., 2000. al., e. Cell motility and shape I: microfilaments, In: Freeman, W.H. (Ed.), Molecular Cell Biology, 4th ed., New York.

Manni, L., Lane, N.J., Joly, J.S., Gasparini, F., Tiozzo, S., Caicci, F., Zaniolo, G., Burighel, P., 2004. Neurogenic and non-neurogenic placodes in ascidians. J. Exp. Zool. B Mol. Dev. Evol. 302, 483–504.

Marti-Solans, J., Ferrandez-Roldan, A., Godoy-Marin, H., Badia-Ramentol, J., Torres-Aguila, N.P., Rodriguez-Mari, A., Bouquet, J.M., Chourrout, D., Thompson, E.M., Albalat, R., Cañestro, C., 2015. Oikopleura dioica culturing made easy: a low-cost facility for an emerging animal model in EvoDevo. Genesis 53, 183–193.

Mayer, Y., Czosnek, H., Zeelon, P.E., Yaffe, D., Nudel, U., 1984. Expression of the genes coding for the skeletal muscle and cardiac actions in the heart. Nucleic Acids Res. 12, 1087–1100.

Mikhaleva, Y., Kreneisz, O., Olsen, L.C., Glover, J.C., Chourrout, D., 2015. Modification of the larval swimming behavior in Oikopleura dioica, a chordate with a miniaturized central nervous system by dsRNA injection into fertilized eggs. J. Exp. Zool. B Mol. Dev. Evol.

Müller, W., 1870. Beobachtungen des pathologischen Instituts zu Jena.

Munro, E.M., Odell, G., 2002. Morphogenetic pattern formation during ascidian notochord formation is regulative and highly robust. Development 129, 1–12.

Munro, E.M., Odell, G.M., 2002. Polarized basolateral cell motility underlies invagination and convergent extension of the ascidian notochord. Development 129, 13–24.

Nakajima, H., Tanoue, T., 2012. The circumferential actomyosin belt in epithelial cells is regulated by the Lulu2-p114RhoGEF system. Small GTPases 3, 91–96.

Nishida, H., 2008. Development of the appendicularian Oikopleura dioica: culture, genome, and cell lineages. Dev. Growth Differ. 50 (Suppl 1), S239–S256.

Nishino, A., Satou, Y., Morisawa, M., Satoh, N., 2000. Muscle actin genes and muscle cells in the appendicularian, Oikopleura longicauda: phylogenetic relationships among muscle tissues in the urochordates. J. Exp. Zool. 288, 135–150.

Olsson, R., 1975. Primitive coronet cells in the brain of Oikopleura (Appendicularia, Tunicata). Acta Zool. 56, 155–161.

Ordahl, C.P., 1986. The skeletal and cardiac alpha-actin genes are coexpressed in early embryonic striated muscle. Dev. Biol. 117, 488–492.

Perrin, B.J., Ervasti, J.M., 2010. The actin gene family: function follows isoform. Cytoskeleton 67, 630–634.

Philimonenko, V.V., Zhao, J., Iben, S., Dingova, H., Kysela, K., Kahle, M., Zentgraf, H., Hofmann, W.A., de Lanerolle, P., Hozak, P., Grummt, I., 2004. Nuclear actin and myosin I are required for RNA polymerase I transcription. Nat. Cell Biol. 6, 1165–1172.

Pollard, T.D., 2010. Mechanics of cytokinesis in eukaryotes. Curr. Opin. Cell Biol. 22, 50–56.

Quarmby, L., 2014. Cilia assembly: a role for F-actin in IFT recruitment. Curr. Biol. 24, R796–R798.

Ramkumar, N., Baum, B., 2016. Coupling changes in cell shape to chromosome segregation. Nat. Rev. Mol. Cell Biol. 17, 511–521.

Roblodowski, C., He, Q., 2017. Drosophila Dunc-115 mediates axon projection through actin binding. Invertebr. Neurosci. 17, 2.

Ronquist, F., Teslenko, M., van der Mark, P., Ayres, D.L., Darling, A., Hohna, S., Larget, B., Liu, L., Suchard, M.A., Huelsenbeck, J.P., 2012. MrBayes 3.2: efficient Bayesian phylogenetic inference and model choice across a large model space. Syst. Biol. 61, 539–542.

Ruan, W., Lai, M., 2007. Actin, a reliable marker of internal control?. Clin. Chim. Acta 385, 1–5.

Ruzicka, D.L., Schwartz, R.J., 1988. Sequential activation of alpha-actin genes during avian cardiogenesis: vascular smooth muscle alpha-actin gene transcripts mark the onset of cardiomyocyte differentiation. J. Cell Biol. 107, 2575–2586.

Satoh, N., 2016. Chapter 7 - The New Organizers Hypothesis for Chordate Origins, Chordate Origins and Evolution. Academic Press, San Diego, 97–120.

Satoh, N., Rokhsar, D., Nishikawa, T., 2014. Chordate evolution and the three-phylum system. Proc. Biol. Sci. 281, 20141729.

Schwartz, K., de la Bastie, D., Bouveret, P., Oliviero, P., Alonso, S., Buckingham, M., 1986. Alpha-skeletal muscle actin mRNA's accumulate in hypertrophied adult rat hearts. Circ. Res. 59, 551–555.

Schwayer, C., Sikora, M., Slovakova, J., Kardos, R., Heisenberg, C.P., 2016. Actin rings of power. Dev. Cell 37, 493–506.

Silva, R.C., Sattlegger, E., Castilho, B.A., 2016. Perturbations in actin dynamics reconfigure protein complexes that modulate GCN2 activity and promote an eIF2 response. J. Cell Sci. 129, 4521–4533.

Soviknes, A.M., Chourrout, D., Glover, J.C., 2007. Development of the caudal nerve cord, motoneurons, and muscle innervation in the appendicularian urochordate Oikopleura dioica. J. Comp. Neurol. 503, 224–243.

Soviknes, A.M., Glover, J.C., 2007. Spatiotemporal patterns of neurogenesis in the appendicularian Oikopleura dioica. Dev. Biol. 311, 264–275.

Soviknes, A.M., Glover, J.C., 2008. Continued growth and cell proliferation into adulthood in the notochord of the appendicularian Oikopleura dioica. Biol. Bull. 214, 17–28.

Suzuki, M.M., Satoh, N., 2000. Genes expressed in the amphioxus notochord revealed by EST analysis. Dev. Biol. 224, 168–177.

Swalla, B.J., White, M.E., Zhou, J., Jeffery, W.R., 1994. Heterochronic expression of an adult muscle actin gene during ascidian larval development. Dev. Genet. 15, 51–63.

Takahashi, H., Hotta, K., Erives, A., Di Gregorio, A., Zeller, R.W., Levine, M., Satoh, N., 1999. Brachyury downstream notochord differentiation in the ascidian embryo. Genes Dev. 13, 1519–1523.

Tomlinson, C.R., Beach, R.L., Jeffery, W.R., 1987. Differential expression of a muscle actin gene in muscle cell lineages of ascidian embryos. Development 101, 751–765.

Tripathi, S.C., 1989. A possible role of actin in the mechanical control of the cell cycle. Biol. Cell 67, 351–353.

Urano, A., Suzuki, M.M., Zhang, P., Satoh, N., Satoh, G., 2003. Expression of muscle-related genes and two MyoD genes during amphioxus notochord development. Evol. Dev. 5, 447–458.

Vandekerckhove, J., Weber, K., 1978. At least six different actins are expressed in a higher mammal: an analysis based on the amino acid sequence of the amino-terminal tryptic peptide. J. Mol. Biol. 126, 783–802.

Vandekerckhove, J., Weber, K., 1984. Chordate muscle actins differ distinctly from invertebrate muscle actins. The evolution of the different vertebrate muscle actins. J. Mol. Biol. 179, 391–413.

Vartiainen, M.K., Guettler, S., Larijani, B., Treisman, R., 2007. Nuclear actin regulates dynamic subcellular localization and activity of the SRF cofactor MAL. Science 316, 1749–1752.

Vicente-Manzanares, M., Ma, X., Adelstein, R.S., Horwitz, A.R., 2009. Non-muscle myosin II takes centre stage in cell adhesion and migration. Nat. Rev. Mol. Cell Biol. 10, 778–790.

Vidaki, M., Drees, F., Saxena, T., Lanslots, E., Taliaferro, M.J., Tatarakis, A., Burge, C.B., Wang, E.T., Gertler, F.B., 2017. A requirement for mena, an actin regulator, in local mRNA translation in developing neurons. Neuron 95, 608–622, (e605).

Woodcock-Mitchell, J., Mitchell, J.J., Low, R.B., Kieny, M., Sengel, P., Rubbia, L., Skalli, O., Jackson, B., Gabbiani, G., 1988. Alpha-smooth muscle actin is transiently expressed in embryonic rat cardiac and skeletal muscles. Differentiation 39, 161–166.

Zaidel-Bar, R., Zhenhuan, G., Luxenburg, C., 2015. The contractome--a systems view of actomyosin contractility in non-muscle cells. J. Cell Sci. 128, 2209–2217.

Zarnack, K., Feldbrugge, M., 2010. Microtubule-dependent mRNA transport in fungi. Eukaryot. Cell 9, 982–990.